

ANALYSIS OF INTERFERENCE
PHENOMENA OBSERVED AT
ETHIO-FINNO OBSERVATORY (EFO)

By
Desalegn Tadesse

**A THESIS PRESENTED TO
THE SCHOOL OF GRADUATE STUDIES
ADDIS ABABA UNIVERSITY
IN PARTIAL FULFILLMENT OF THE REQUIREMENTS
FOR THE DEGREE OF
MASTER OF SCIENCE in PHYSICS
ADDIS ABABA, ETHIOPIA
JULY 2006**

ADDIS ABABA UNIVERSITY

DEPARTMENT OF PHYSICS

The undersigned hereby certify that they have read and recommend to the Faculty of Science for acceptance a senior project entitled **“ANALYSIS OF INTERFERENCE PHENOMENA OBSERVED AT ETHIO-FINNO OBSERVATORY (EFO) ”** by **Desalegn Tadesse Master of Science.**

Dated: July 2006

Supervisor:

Dr. Baylie Damtie

Readers:

ADDIS ABABA UNIVERSITY

Date: **July 2006**

Author: **Desalegn Tadesse**

Title: **ANALYSIS OF INTERFERENCE PHENOMENA OBSERVED
AT ETHIO-FINNO OBSERVATORY (EFO)**

Department: **Deaprnment of Physics**

Degree: **M.Sc.** Convocation: **July** Year: **2006**

Permission is herewith granted to Addis Ababa University to circulate and to have copied for non-commercial purposes, at its discretion, the above title upon the request of individuals or institutions.

Signature of Author

to boche

Table of Contents

Table of Contents	v
List of Tables	vii
List of Figures	viii
Acknowledgements	xi
Abstract	xii
1 General introduction	1
1.1 Sources of the Earth Magnetic field	2
1.2 Internal Sources	2
1.2.1 Core Originated Field	2
1.2.2 Field from the Lithosphere	3
1.2.3 Field from Earth Rotation	6
1.3 External Sources	6
1.3.1 Ionospheric Field	6
1.3.2 Magnetospheric Field	6
1.3.3 Field Aligned Coupling Current	7
1.4 Variations in the Earth Magnetic Field	9
1.4.1 Secular Variations	9
1.4.2 Temporal Variations	9
1.5 Magnetic Storm	10
1.6 Magnetospheric Substorm	11
1.7 Man-made Disturbances	13
1.8 Pulsations of the Earth Magnetic Field by ULF Waves	13
1.9 Parametrization of Earth Magnetic Field	15
2 Measuring the Earth magnetic field	18
2.1 Introduction	18
2.1.1 Compass	19
2.1.2 Flux-gate Magnetometer	19
2.1.3 Proton Precession Magnetometer	20

2.1.4	The absorption-cell Magnetometer	21
3	The Ethio-Finno Observatory (EFO)	23
3.1	Instrumentations	23
3.1.1	Sensors at EFO	23
3.1.2	Analogue Electronics	24
3.1.3	Digital Electronics	25
3.1.4	Host Pc	25
4	Measurement and Data Analysis	26
4.1	Data from EFO and Observed Interference	26
4.2	Investigations of the Possible Sources of the Interference	31
4.2.1	Solar and Geomagnetic Effect	31
4.2.2	Effect of Ferrous Objects	32
4.2.3	Errors from Ground Loop Effect	37
5	Conclusions	42
6	Future directions	43

List of Tables

1.1 Summary of the ULF waves kinds, their corresponding periods and frequencies.	14
--	----

List of Figures

1.1	The alpha-omega dynamo cycle: consider an initial dipolar poloidal field, such as in (a). The omega-effect consists of (b,c) rotation differential rotation, wrapping the magnetic field around the rotation axis, thereby creating (d) a quadrupolar toroidal magnetic field. inside the core. A closure of the dynamo cycle requires a bit of symmetry breaking, brought about by the alpha-effect, where by (e) helical up welling and down welling creates loops of magnetic field. These loops cause (f) to reinforce the original dipolar field.	4
1.2	Left panel: Three-dimensional structure of the core magnetic field; the field has a complicated form in the inside the core but exhibits a nearly dipolar structure outside the core. Right panel: The axial dipolar part of the Earth's magnetic field, with field lines emanating from near the south geomagnetic pole and concerning near the north geomagnetic pole. The dipolar part of the field is actually tilted by approximately with the rotational axis.	5
1.3	Schematic diagram of the electric-current pattern in the ionosphere driven by diurnal heating from the sun. The current is connected on the day side, consisting of two oriented circuits.	7
1.4	A schematic diagram depicting the magnetosphere in the near-Earth space environment. The southward orientation of the interplanetary magnetic field, and the reconnection process with the geomagnetic field that follows as the solar wind carries the interplanetary field the past the Earth.	8

1.5	A stack point of horizontal field intensity (H) as measured by eleven USGS chain observatories magnetometer during the great storm of March 1989.	12
1.6	The geomagnetic field can be described by north(X), east(Y) and vertically downward(Z) cartesian components, or by the angles of declination(D) and inclination(I) together with the total field intensity(F).	16
3.1	Instrumental setup of ionospheric monitoring at EFO triaxial pulsation magnetometer positioned on plane surface	24
4.1	The H-component of the four days Feb 15-18, 2005 geomagnetic disturbance recorded at EFO.	27
4.2	The dynamic spectrum in a color code as a function of frequency and time as observed at EFO from the first one hour of the four days. The ordinate displays frequency in Hz and the tick mark abscissa indicates the time. Deep red of the color code corresponds to plus ~ 0.6 and deep blue to minus ~ 0.6	28
4.3	Three components of the quasi-periodic disturbances which persists for less than 0.5 seconds. The color code shows on the vertical axis frequency content and the horizontal axis time.	29
4.4	Three components of the sharp pulse quasi-periodic disturbances which persists for less than 0.85 seconds. The color code shows on the vertical axis frequency content and the horizontal axis time.	30
4.5	Sample of long persisting disturbances of the three components. The dynamic spectrum indicates the disturbance possess frequency 0-50Hz.	30
4.6	Upper panel: indicates disturbance on February 18, 2005 due to minor storm. Lower panel: is the frequency content of the disturbance in color code.	31
4.7	Ferrous object disturbance in uniform field.	33
4.8	Direction sensing for ferrous disturbance moving over magnetic sensors.	33
4.9	Disturbance created during the vibration of the wire fence near the sensors.	34

4.10	Left column indicates Earth's field variations for car (silhouette) driving over the magnetometer. Right column is due to car (saturn). Both vehicle are travelling in the same direction (16).	35
4.11	Left column the X, Y, and Z magnetic variation from a car in the forward(south) and reverse (north) and right column forward (west) revers (east) direction (16).	36
4.12	A simplified ground loop producing circuit.	39
4.13	A sharp pulse created while moving the divider or unplugging the power cable after the divider. This is the disturbance expected if the grounding current loops doesn't exist in close the magnetometer and its parts. . . .	40
4.14	Observed disturbance and corresponding frequency content during ground- ing current loops source test is held near the UPS.	41
4.15	Observed disturbance and corresponding frequency content while ground- ing current loops source test is held near the sensors.	41

Acknowledgements

I am deeply grateful to my supervisor Dr. Baylie Damte with all his effort who introduced me space physics and simulation. He has been an endearing friend and perceptive advisor in dealing with ingredients pertaining to these thesis. I would like also to thank Dr. Mulugeta Bekele former A.A.U. Physics Department head, Dr. Tilahun Tesfaye A.A.U. the present Physics Department head who arranged conditions to work with my advisor, and A.A.U. Graduate Program for the extensive support. I am specially grateful to Bahir Dar University Post Graduate Research Program for helping a lot by supplying me personal computer access that simplified my work.

In addition I would like to express my appreciations to Dr. Endawoke Yezenga who gave me great help in locating reference for data, and figures in relation to my work.

And I finally want to thank my brothers hilariously letting me devote so much time in this work.

Addis Ababa University

Desalegn Tadesse

June, 2005

Abstract

The pulsation magnetometer at Ethio-Finno Observatory (EFO) has been operational since June 2004. The major objectives of this instrument is to characteristically investigate the ionospheric phenomena of the upper polar atmosphere. Results from the data analysis in time and frequency domain depicts existence of strong interferences which are not observed in other similar observatories. In this thesis we shall investigate the disturbance characteristics and delve out the cause of peaks by relating with solar activities, geomagnetic activities and local effects such as ferrous object, and ground loop. This is done by carefully investigating the data collected during some days and by conducting controlled experiment.

Preface

To be able to observe remotely the earth magnetic field disturbances in the ionosphere and magnetosphere that presents impressive experiences in human understanding of the natural process of the upper polar atmosphere we use compasses and magnetometers. These devices are rapidly growing with the advancement of technology and they are now widely applicable on Earth surface, sea, aeroplanes, space vehicles and satellites. In order to better relates data furnished from such instruments it is found out that establishment of new observatories in all over the globe is inevitable.

In this thesis we have aimed to study the characteristics and to sort out the cause of strongly enhanced disturbance obtained from ionospheric monitoring observatory EFO data by relating with solar and geomagnetic activities, ferrous materials influences and grounding current loops noises from the near by locations.

Chapter one is devoted to deal with sources, causes and characteristics of the Earth's magnetic field. Wide range of coverage for Earth magnetic field measurement and measuring instruments used is given in chapter two. Detail description of EFO and instruments is given in chapter three. Analysis of the cause of interferences at EFO is discussed in chapter four which is the theme of this thesis. The last two chapters incorporates conclusions and future directions respectively.

Chapter 1

General introduction

Exploration of magnetism and magnetic phenomena began due to the attractive properties of lodestone. The Chinese around 300 B. C were using suspended and pivoted-needle compasses that aligns to specific direction for navigation. William Gilbert in 1600 showed that this properties is due to the Earth itself posses a magnetic character; acts as a great magnet (" De Magnet "). For further investigation of geomagnetism he initiated the idea for continuous recording and establishing many observatories. After that proper recording of Earth magnetic field began which nearly accounts about five century now.

Continuous recording of Earth magnetic field gives the base for scientists and researchers to propose hypothesis and lead in the development of many plausible theory in explaining the possible sources of the Earth magnetic field. More analysis like comparisons of different time data reveals that the Earth magnetic field is exposed for temporal variations. These variations occur over wide spectrum, with periods ranging sub-milliseconds to tens of millions of years (13). Geomagnetic variations which are secular type have internal origin, caused by fluid motion in the Earth's liquid iron outer core. The time scale of this field is of the order of centuries (11). The short term geomagnetic field variations are attributed by external originated disturbance, ionospheric and magnetospheric (14). The level of variation for the short term is time dependent. Such fact is related to the intensity of solar wind phenomena related to the dynamic process in the sun.

During high solar activities, large number of solar flare and corona holes are

formed, the solar wind magnetic field (IMF) orients antiparallel to the earth's main field that will be felt as a bow shock or disturbance. Intensified distortions such as magnetic storms geomagnetically induced current (GIC) in technological devices and creates human affecting phenomenon (11), (12): like increase radiation doses for occupants of transport flight, distortion of compass reading in polar regions, disrupting of shortwave radio communications, increased corrosion in long pipelines, failure of electrical transmission lines, anomalies in the operations of communications satellites, Global positioning systems (GPSs) can be degraded, and potentially lethal doses of radiation for astronauts to interplanetary space craft.

Nowadays we have more understanding of the Earth magnetic field based on observations by means different kinds of modern magnetometers and advanced computer assisted simulations. This device are employed on Earth's surface over 200 observatories. There is also, in-situ measurements by space vehicles, aeroplanes and many satellites. Records from all these observatories indicates the total Earth magnetic field intensity is in the range 30000nT in the equator and 60000nT at the poles. Off all the total field the 99 per cent is originated from the internal source. The rest of magnetic field (about one percent) originates from the external source.

Despite significant effort to understand it, geomagnetic process remains enigmatic. For more better understanding of the Earth's upper polar ionosphere, it is indispensable to introduce new observatories all over the world, such as the EFO that operate in Ethiopia.

In this thesis, we start with the detailed descriptions of the Earth magnetic field and proceed on the measurement of pulsation of Earth magnetic field and finally we will delve out the cause of unknown fluctuation observed at EFO.

1.1 Sources of the Earth Magnetic field

1.2 Internal Sources

1.2.1 Core Originated Field

The Earth core is set off from the mantel by a very sharp boundary. The core has a diameter of 7000Km. Approximately 1200km of the core is made of solid sphere of

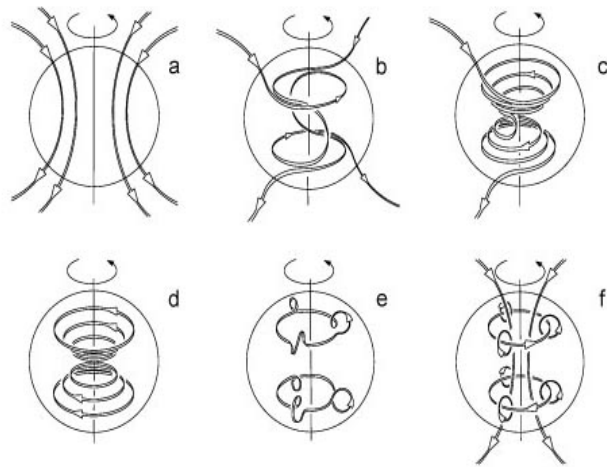
iron surrounded by liquid core. The temperature of the core is close to 4000 degree Celsius. The thermal heating due to these very high temperature in the core drives the fluid into motion. According to the dynamo theory, fluid motion in the core moves conducting materials across an existing magnetic field. This field interacts with fluid motion to create a secondary magnetic field with the same orientation as the original field. The two fields together are stronger than the original in there intensity (3), (12).

Depending on the geomagnetic relationship between the fluid flow and the magnetic field, the generated magnetic field can reinforce the pre-existing magnetic field, in which case the dynamo is said to be 'self-sustaining'. These behavior of the Earth magnetic field is depicted by kinematics stand point the so called Coriolis force, consists of a combination of different rotation and convection, turbulent helical motion. The alpha-omega process successfully describes how it is that the magnetic field can be amplified, but it is the dynamics that ultimately determines the field's strength; the field grows with rough balance is attained between the Coriolis and the Lorentz force (6) (see Figure 1.1).

The measurement of Earth magnetic field on surface indicates the core originated field accounts about 97 per cent of the total field. The intensity ranging about 30000nT at the equator and about 50000nT at the poles (8). Thus the magnetic field of the Earth is often times described by being approximately dipolar, with field lines emanating from south geomagnetic pole and converging at the north geomagnetic pole, as depicted in the left panel of Figure 1.2.

1.2.2 Field from the Lithosphere

Field from lithosphere is due to the magnetization of rock of the Earth. The magnetization of the rock on the Earth due to the Earth's magnetic field is called crustal magnetization. Basically two types of crustal magnetic field exists, induced and remanent (permanent). The former one occurs when the elementary magnetic dipoles of crustal materials are aligned by the Earth's main field. The magnetization is proportional to the intensity of the ambient field and vanishes when the primary field vanishes. The latter one is similar to induced magnetization, but once created it persists after the primary field has disappeared. Field from Earth rock magnetization have recorded effect of amplitude up to several thousands nT at the surface and at



Love, J. J., 1999. *Astronomy & Geophysics*, 40, 6.14-6.19.

Figure 1.1: The alpha-omega dynamo cycle: consider an initial dipolar poloidal field, such as in (a). The omega-effect consists of (b,c) rotation differential rotation, wrapping the magnetic field around the rotation axis, thereby creating (d) a quadrupolar toroidal magnetic field. Inside the core. A closure of the dynamo cycle requires a bit of symmetry breaking, brought about by the alpha-effect, whereby (e) helical upwelling and downwelling creates loops of magnetic field. These loops cause (f) to reinforce the original dipolar field.

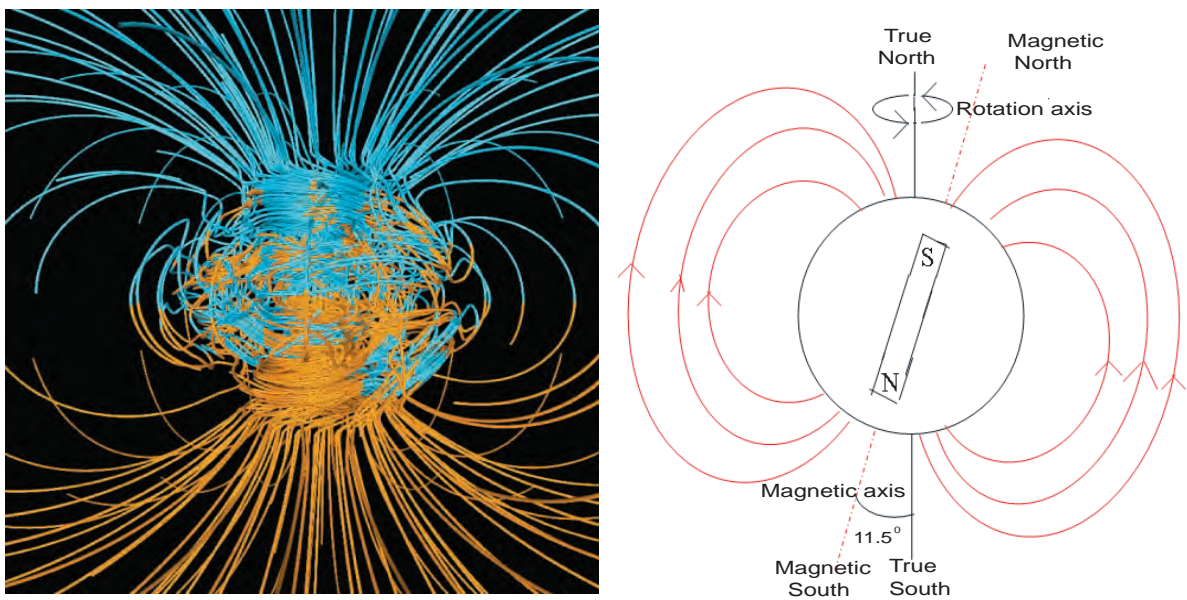


Figure 1.2: Left panel: Three-dimensional structure of the core magnetic field; the field has a complicated form in the inside the core but exhibits a nearly dipolar structure outside the core. Right panel: The axial dipolar part of the Earth's magnetic field, with field lines emanating from near the south geomagnetic pole and concerning near the north geomagnetic pole. The dipolar part of the field is actually tilted by approximately with the rotational axis.

air craft altitude, and up to about 20nT at the satellite altitude (7).

1.2.3 Field from Earth Rotation

As the interior of the earth is extremely hot and the fluid part is serving as a highly conducting plasma. The rotation of fluid is supposed to create a rotation cell in the interior which gives rise to a current that induces a magnetic field. Due to a gyroscopic effects causes a partial lining of the magnetic moment along the Earth's axis of rotation. The magnetization arising due to the rotation is about 10^{-6} nT (3). This small value is attributed because the Earth angular velocity is very low.

1.3 External Sources

1.3.1 Ionospheric Field

The wind from the sun disturbs the ionosphere current system by heating the day side and cooling the night side as shown in Figure 1.3. This generates a tidal wind that drives ionospheric plasma against the geomagnetic fields and current dynamo. Since the geomagnetic field is strictly horizontal at the dip equator, there is an enhancement of the effective conductivity. This results in an enhanced eastward current, called the equatorial electrojet, that flows on the dayside of dip equator (5). In addition, auroral electrojet flow in the auroral belt and vary in amplitude with different levels of magnetic activity.

At the Earth's surface, during quiet day fields are of the order 10-50nT, depending upon components, latitude, season, solar activities and time of day. The magnetic signature of the equatorial electrojet can be 50-500nT; and that of the auroral electrojet vary widely from a few 10snT during quiet periods to several thousands nT during major magnetic storm (17).

1.3.2 Magnetospheric Field

The field originating in the Earth's magnetosphere is a result primarily of the ring-current and the the current on the magnetopause and in the magnetotail. Currents

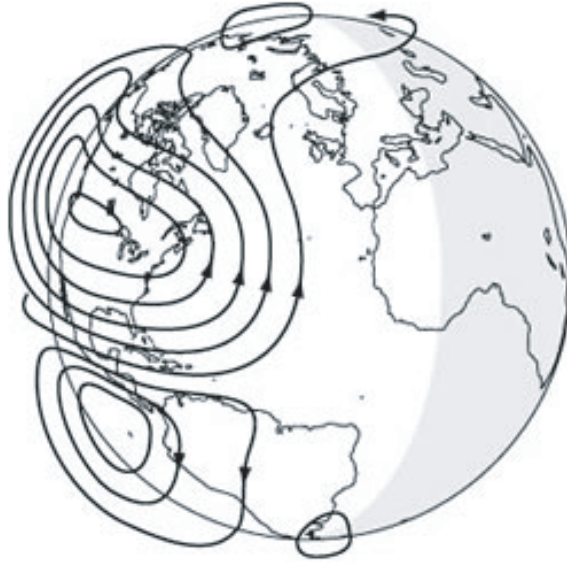


Figure 1.3: Schematic diagram of the electric-current pattern in the ionosphere driven by diurnal heating from the sun. The current is connected on the day side, consisting of two oriented circuits.

flowing on the outer boundary of the magnetospheric cavity, known as the magnetopause, cancel the Earth's field outside and distort the field within the cavity. This produces an elongated tail as indicated in Figure 1.4 antisolar direction within which sheet currents are established in the equatorial plane. The interaction of these currents with the radiation belts near the Earth produces a ring-current in the dipole equatorial plane. These ring-current attains a field-aligned currents into and out of the ionosphere. These resulting broad-scale fields having magnitude of the order of 20-30nT during magnetically quiet periods, but can increase to several hundred nT during disturbed times (6).

1.3.3 Field Aligned Coupling Current

Most of the current densities associated with the external fields have solenoidal character. Hence flow along closed circuits. Due to the the complex nature of the conductivity structure in the earth upper regions, circuit closure is sometimes achieved through that coupling the various source.

At high latitudes, the auroral ionosphere and magnetosphere are coupled by the

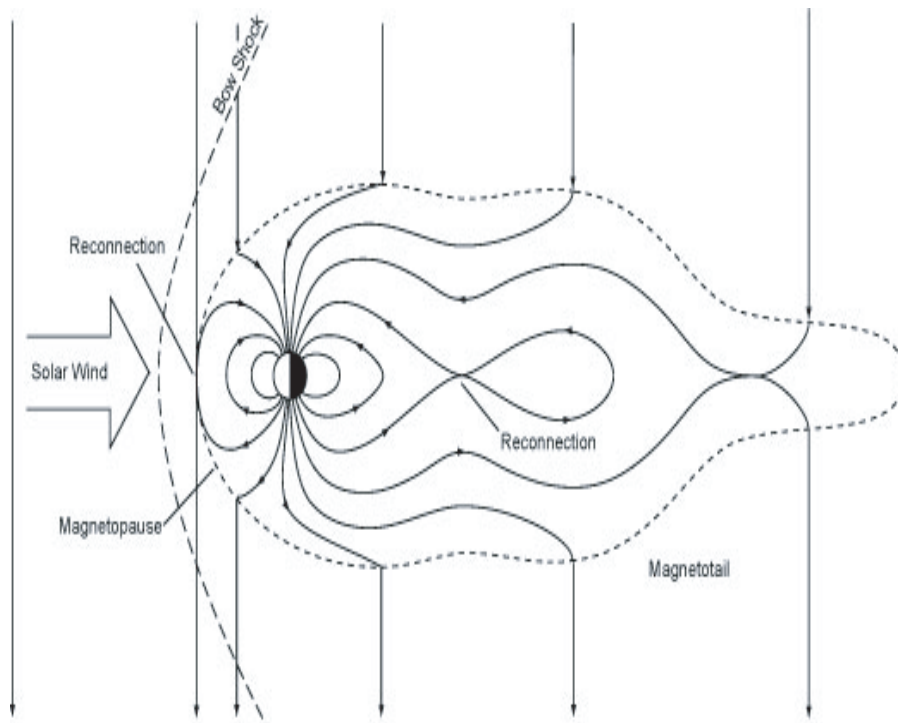


Figure 1.4: A schematic diagram depicting the magnetosphere in the near-Earth space environment. The southward orientation of the interplanetary magnetic field, and the reconnection process with the geomagnetic field that follows as the solar wind carries the interplanetary field the past the Earth.

currents that flow along the Earth's magnetic field lines. The field from these field-aligned currents have magnitudes that vary with the magnetic disturbance level (18). However, they are always present of the order of 30-100nT during quiet periods and up to several thousand nT during substorms. There are also currents that couple the solar quiet currents systems in the two hemispheres along the magnetic field lines. The associated magnetic fields are generally 10nT or less. Finally, there exists a meridional current system that is connected to the equatorial electrojets with upward-directed currents at low latitudes. Fields from this current system resulted about 15-40nT (19).

1.4 Variations in the Earth Magnetic Field

It is clear that Earth's magnetic field is not constant. It continuously changes and shows fluctuation due to perturbation from external interference and the dynamic process in internal part. Basically two distinct types of changes are observed; transient fluctuation and long term secular changes.

1.4.1 Secular Variations

Secular variation is loosely used to indicate slow changes with time perhaps one year and longer. These variations are the manifests as changes of both the dipole and non dipole components of the Earth's magnetic field. Such variations include change in field intensity, orientations of the main field, and westward drift of the main field (inclination and declination). All this changes result a net considerable impact on the Earth's main field (21). However, the cause and the source of secular variation is still under debate. The possible theories suggested are discussed in detail in (12).

1.4.2 Temporal Variations

The continuous magnetic records of any observatory shows that on some days all the three elements exhibits smooth and regular variations, while on the other days they are disturbed and shows irregular fluctuations. Such variation are termed as temporal or transient variations which are examined in 3-h Kp indices and Dst values

terms of variation. This variation do not produce enduring change on the Earth's main field (3). The source for temporal variation is caused by out side from the Earth.

The ionized molecules in the ionosphere releases swarms of electrons that can acts as a source of external magnetic fields. As the Earth rotates the perturbation of the geomagnetic field by the external causes fluctuation in intensity of amplitude ranging from 10-30nT at the Earth surface. Since the intensity of the ionization depends on the state of solar activities so as the degree of fluctuation. For instance during sunspot and solar flares strong magnetic fields called magnetic storms (discussed more in section 1.5) with amplitude up to 1000nT at the Earth's surface are recorded. In addition to large scale geomagnetic variations, there are disturbance of much shorter duration. Abrupt impulsive changes may also occur, while variation with periods roughly ranges from 0.1s to 10min are grouped together and called geomagnetic pulsation (see section 1.8).

1.5 Magnetic Storm

Magnetic storm is an interval of several days duration which there is a large reduction in the horizontal component of the surface magnetic field (12). The most spectacular events that may cause a magnetic storm is a solar flare, and existence of coronal holes around the sun. This attributes sudden increase in the dynamic pressure of the solar wind as high speed and high density plasma from the sun suddenly arrive at Earth. The leading edge of this region reaches the Earth and passes the magnetopause Earthward. The sudden eastward motion and accompanying increase in strength of the magnetopause current cause an abrupt increase in the magnetic field at the Earth's surface known as the storm sudden commencement. In most cases, the pressure remains high for a number of hours and causes a large than normal surface field. This interval is called initial phase of a magnetic storm. The main phase is cause by the growth of a ring current around the Earth that drifts westward. This current is primarily created by ions including protons, helium, and oxygen drifting westward around the Earth from midnight towards dusk and onward. This current act much like a large solenoid around the Earth producing a magnetic disturbance that is southward along the Earth's dipole axis. The recovery phase of the storm is

caused by the loss of these ions. As the ions approach the atmosphere in their bounce motion there is a high probability of interaction with an atmospheric neutral atom. An electron from the cold atmosphere is exchanged with the hot ion. The hot ion becomes an energetic neutral atom that is no longer confined by the field .

The creation of the ring current is caused by a prolonged interval of strong southward magnetic field and high solar wind velocity. These are precisely the conditions that cause magnetic reconnection on the dayside and intense convection in the magnetosphere. The ions creating the current are brought in from the tail and energized by the magnetospheric electric field associated with convection. These field drifts the ionized particles faster close to the Earth enhances the nightside ring current and reduces the magnetic field on the Earth's surface.

1.6 Magnetospheric Substorm

Magnetospheric substorm is the name applied to the collection of processes that occur throughout the magnetosphere at the time of an auroral and magnetic disturbance (21). A substorm is distinct from magnetic storm the events being localized in time and space. The events typically last around three hours and occur 3-6 times per day. During substorm a large amount of energy is extracted from the solar wind and is dumped into the magnetosphere and ionosphere. The substorm is characterized by three phases; growth, expansion, and recovery.

The growth phase begins when the solar wind magnetic field turns southward and magnetic reconnection begins at the subsolar magnetopause. During this phase the size of the polar caps grows as more magnetic field lines are connected to the polar wind. The open field lines enable the solar wind electric field that points from dawn to dusk to be transmitted to the ionosphere. Current derived by the field flows along the auroral oval towards midnight. On the dawn side this portion of the current is called the westward electrojet. On the dusk side it is called the eastward electrojet. The growth phase persists for about an hour and is terminated by a sudden brightening and activation of the most equatorward arc. This signifies the beginning of expansion phase.

Soon after onset, auroral activities expand to fill the entire sky. Rapid motion,

12-18 March 1989 Horizontal intensity

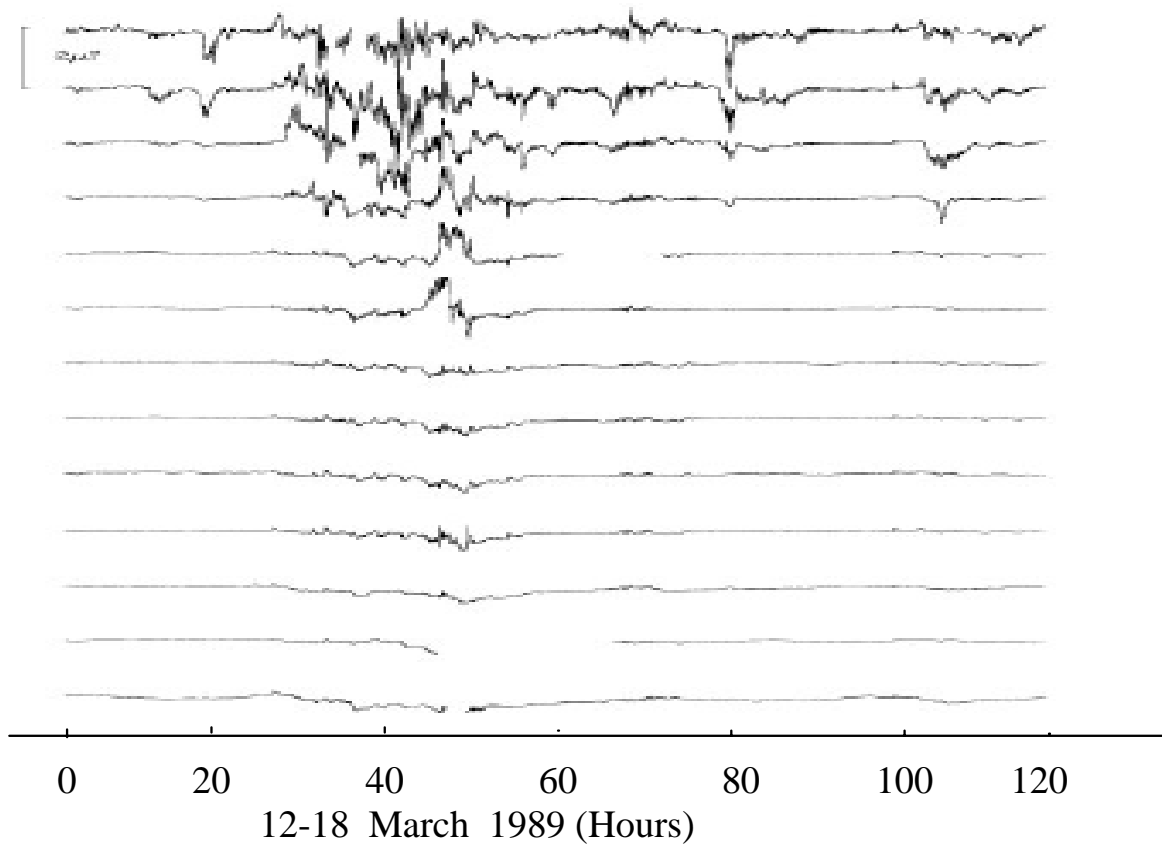


Figure 1.5: A stack point of horizontal field intensity (H) as measured by eleven USGS chain observatories magnetometer during the great storm of March 1989.

developed of vertical rays and folds, color at the bottom of auroral forms. This phenomena expands polarward and westward. A surge of bright aurora propagates to the west which enhances the electrojet as a result the ground magnetic field suddenly decreases and patches of pulsation aurora and large omegashaped bands drift eastward. This process continues for about 30-40 minutes the x-lines begins to move down the tail. This signals the beginning of recovery phase.

The fine phase of a substorm is called the recovery phase. During this phase the aurora and current gradually drift back to their original equatorward locations as they simultaneously decrease in luminosity and strength. This last after approximately 90 minuets.

1.7 Man-made Disturbances

Nuclear explosions, particularly in the upper atmosphere, perturb the magnetic field. A chemical explosions of considerable strength is also capable provoking a noticeable reaction in the ionosphere. Explosions of lesser strength are also capable of provoking considerable modification to the environment and deform the spectrum of natural electromagnetic radiations if they follow each other for a long period of time. Artificial perturbation of such kind distorts geoelectromagnetic backgrounds.

In addition the geomagnetic wave is perturbed by functioning of technical devices (radiometers, electric power lines, DC-power rapid transient system, etc.) (20). The major argument of this kind of device has been investigated in the so called weekend effect. It turns out that on Saturday and Sunday, when the industrial activity calms down every where, total geomagnetic activity increases as compared to other days of the week (20). This gives the impression that industrial activity suppresses the activity of the magnetosphere or rather suppresses the kinds of activities that form the weekend effect.

1.8 Pulsations of the Earth Magnetic Field by ULF Waves

The magneto hydrodynamics (MHD) waves originated in the outer magnetic field superimpose along field lines to the Earth surface. This will create resonant oscillation

pulsation	period	frequency
Pc-1	0.2-5(s)	0.2-5(Hz)
Pc-2	5-10(s)	0.1-0.2(Hz)
Pc-3	10-45(s)	22-100(mHz)
Pc-4	45-100(s)	7-22(mHz)
Pc-5	50-600(s)	2-7(mHz)
Pi-1	1-40(s)	0.025-1(Hz)
Pi-2	40-150(s)	1-25(mHz)

Table 1.1: Summary of the ULF waves kinds, their corresponding periods and frequencies.

that characterizes the geomagnetic pulsations; a class of electromagnetic waves ultra-low-frequency (ULF) plasma (12), (20). These waves, in the Earth's magnetosphere, have frequency ranging from approximately one megahertz to greater than ten hertz. They appear as quasi-sinusoidal oscillation in magnetometer data recorded at the Earth's surface, ionosphere and magnetosphere. The lowest frequency pulsations have the largest amplitude the high-frequency pulsations have the amplitude which are greater than several nanotesla, and typically have less than on the Earth's surface.

Magnetic pulsation are classified phenomenologically on the basis of waveform into pulsation continuous (Pc) and pulsation irregular (Pi). Pc are quasi-sinusoidal in form and each with well-defined spectral peak. Pi are in the same frequency band contained power at many different frequencies. Each class is subdivided into different frequency bands on the basis of boundaries defined by different generation mechanism and their periods. Table 1.1 gives brief summary of ULF waves with the periods and frequency.

Continuous pulsation in the lower-frequency band (1mHz to 10mHz) are caused predominantly by hydromagnetic instability. Such as the Kelving-Helmholz and drift-mirror instability. Many pulsation in the mid-frequency band (10mHz to 0.1Hz) are originated from proton cyclotron instability in the solar wind, which propagate through the magnetosphere. Continuous pulsation in the higher-frequency band (0.1 to 10Hz) generally are caused by ion cyclotron instabilities in the magnetosphere.

Impulsive pulsation (Pi) are caused by a variety of transient phenomena, including

sudden impulse from the solar wind, flux transfers, and rapid change in magnetospheric convection. Shocks and discontinuities in the solar wind produce the sudden impulses which propagate as fast Alfvén models in the magnetosphere. Transient and localized reconnection or flux transfer events on the dayside of the magnetopause propagate along field lines giving field-aligned current system and transient pulsation which appear to be propagating in an antisunward direction. The substorm expansive phase makes sudden changes in the convection and the release of energy in the magnetotail. Much of this energy is carried transient field-aligned current. These field-aligned currents propagate as shear Alfvén waves which can be seen in the nightside magnetosphere and on the ground.

1.9 Parametrization of Earth Magnetic Field

The Earth magnetic field can be parameterized by using vector. It can be expressed as cartesian components parallel to any three orthogonal axes (X,Y,Z). The geomagnetic elements are taken to be components parallel to the geographic north and the east direction and the vertically down ward direction as shown in Figure 1.9. Alternatively, we can also use spherical polar coordinates. The magnitude of the magnetic vector is given by the field-strength F ; its direction is specified by two angles. The declination D is the angle between the magnetic meridian and the geographic meridian. The inclination I is the angle at which the magnetic vector dips below the horizontal (Figure 1.9). From the point observation the earth magnetic field B and its potential V at the any point can be expressed in terms of the spherical polar coordinates (r, θ, ϕ) . According to (9) the magnetic field is derived as the the negative gradient of the scalar potential that is

$$B = -\nabla V \tag{1.1}$$

According to (6) the magnetic scalar potential can be expressed in the terms of spherical harmonics of different sources as

$$\begin{aligned}
V = & a \left\{ \sum_{n=1}^{\infty} \sum_{m=0}^n (g_n^m \cos m\pi + h_n^m \sin m\pi) \left(\frac{a}{r}\right)^{n+1} P_n^m(\cos \theta) + \right. \\
& \sum_{n=1}^{\infty} \sum_{m=0}^n (\dot{g}_n^m \cos m\pi + \dot{h}_n^m \sin m\pi) \left(\frac{a}{r}\right)^{n+1} (t - t_o) P_n^m(\cos \theta) + \\
& \sum_{n=1}^{n=2} \sum_{m=0}^n n (q_n^m \cos m\pi + s_n^m \sin m\pi) \left(\frac{a}{r}\right)^n P_n^m(\cos \theta) + \\
& \left. \tilde{RC} \left[\left(\frac{r}{a}\right) + Q_1 \left(\frac{a}{r}\right)^2 \right] \times [\tilde{q}_1^0 P_1^0(\cos \theta) + (\tilde{q}_1^1 \cos \phi + \tilde{s}_1^1 \sin \phi) P_1^1(\cos \theta)] \right\}, \quad (1.2)
\end{aligned}$$

where a is the mean radius of the Earth, $P_n^m(\cos \theta)$ are the associated Schmidt semi-normalized Legendre functions of degree n and order m , and (g_n^m, h_n^m) and (q_n^m, s_n^m) are the Gauss coefficients describing sources internal and external to the Earth, respectively. $(\dot{g}_n^m, \dot{h}_n^m)$ describe the (linear) secular variation around a given epoch t_o . In addition, the $n = 1, 2, m = 0$, terms incorporated an annual and semi-annual variation. The last part of the above equation (coefficients \tilde{q}_1^0 , \tilde{q}_1^1 and \tilde{s}_1^1) accounts for the variability of contributions from the magnetospheric ring current (as measured by \tilde{RC}) plus their internal, induced counterpart. These induced contributions are considered by means of the factor Q_1 .

Chapter 2

Measuring the Earth magnetic field

2.1 Introduction

The Earth magnetic field being due to from internal and partly from external sources that extends more than twenty times Earth's radius makes it to experience a broad spectrum of characteristics and this often makes Earth magnetic field measuring devices in specific location to be unaware the actual phenomena taking place in another area. Hence it is barely possible to deduce about the Earth magnetic field from a single or very small number of measurements. More versatile observation or multidirectional surveying are required. This is done recording data from the Earth surface, oceans, sea, and space.

Measurement of the Earth magnetic field is during earlier time was done commonly by compasses. Most compass operation is mechanical. But for optimum sensitivity and to measure changes in a selected components of the magnetic fields now compasses are more superseded by more delicate, robust electronics instruments called magnetometers. The most important of this is the flux-gate, proton- precision, and optically pumped magnetometer (21).

2.1.1 Compass

Compass is the simplest device used in measuring the Earth magnetic field. It consists of permanently magnetized needle that is balanced to pivot in the horizontal plane. The magnetic sensor alignment determines the component magnetic field to be measured. When a magnetic needle is exposed to magnetic field where the gravitational field is negligible the magnetized needle align itself exactly along the magnetic field vector. This case assists to measure the horizontal field component. The magnitude of the horizontal field is measured from oscillations of the compass needle. The oscillation depends on properties of the needles and the strength of the field. A magnetized needle may also be pivoted and balanced about a horizontal axis. If this needle, called a dip meter, is first aligned in the direction of the magnetic meridian as defined by a compass, the needle lines up with the total field vector and measures the inclination angle I .

Compass can be employed in continuous recording of the earth magnetic field. When a magnetized needles with reflecting mirrors are suspended by quartz fibres, light beams reflected from the mirror are imaged on a photographic negative mounted on a rotating drum. Variations in the field causes corresponding deflections on the negative. Typical scale factors for this method corresponds to 2-10nT per millimeter vertically and to 20 millimeter per hour horizontally. A print of the developed negative called a magnetogram.

2.1.2 Flux-gate Magnetometer

The flux-gate magnetometer works on the the principle Faraday's laws of electromagnetic induction (21). The sensor in this device is designed using two parallel strips of alloys have very low remanent magnetization. They are wound in opposite directions with primary energized coil. When the axis of the sensor is aligned with the earth's magnetic field, the latter is added to the primary field in one strips and subtracted from it in the other. The phase of the magnetic flux in the alloy trips becomes different; one saturates before the other thus the flux-changes in the two alloys strips will no more be equal and opposite. Therefore an out put voltage is produced in the secondary coil that characterizes the Earth's magnetic field along the direction of the

sensor. According to (1) this voltage is related with magnetic field by

$$V_{out} = nAB_{ex}(1 - D)(d\mu_e/dt)/[1 + D(\mu_t - 1)]^2, \quad (2.1)$$

Where V_{out} is the output voltage, n is the number of turning coil, A is the cross-section area, B_{ex} the external magnetic field, μ_e is the effective permeability, D is the demagnetizing factor and μ_t is the relative permeability.

The flux-gate magnetometer is a vector magnetometer, because it measures the strength of the magnetic field in a particular direction i.e. along the axis of the sensor. For total field measurement three sensors are employed. These are fixed at right angles to each other and connected with a feedback system which rotates the entire unites so that two of the sensor detect zero field.

The flux-gate magnetometer does not yield absolute field values. The output is a voltage, which must be calibrated in terms of magnetic field. However, the instrument provides a continuous record of field strength. The portability makes it in wide use of surveying.

2.1.3 Proton Precession Magnetometer

The proton-precession magnetometer is so named because it utilizes the quantum-mechanical precession of spinning protons or nuclei of the hydrogen atom in a sample of hydrocarbon fluid shows when exposed for magnetic field (21). The spinning proton rich liquid in the sensor is such as water, kerosine, alcohol, etc . Around the flask are wound a magnetized solenoid and a detector coil. When the current in the magnetized solenoid is switched on, it creates a magnetized field of the order of 100mT, which is about 2000 times stronger than the Earth's field. The magnetized field aligns the magnetic moments of the proton along the axis of the solenoid, which is oriented approximately east-west at right angle to the Earth's field. The motion of the proton magnetic moments along the ambient magnetic field induces a signal in the detector coil. The induced signal is amplified electronically and the Lamor precessional frequency is accurately measure by counting cycles for a few seconds.The

output frequency f measured is associated with the total magnetic field B_t by

$$B_t = \frac{2\pi}{\gamma_p} f \quad (2.2)$$

The proton-precession magnetometer measures the total absolute magnetic field. Accurate measurement of the signal frequency gives an instrumental sensitivity of about 1nT, but requires a few seconds of observation; continuous record is not possible. Its portability and simplicity give it the advantage for field use like magnetic surveying. Its sensitivity of less than 1nT makes it capable of measuring most magnetic anomalies of the geophysical interest. In contrast to the flux-gate instrument, which measures the component of the field its axis, the proton-precession magnetometer cannot measure field components; it is a total-field magnetometer.

2.1.4 The absorption-cell Magnetometer

The absorption-cell magnetometer is also referred as the alkali-vapor or optically pumped magnetometer. The principle of its operation is based on the quantum-mechanical model of the atoms (21). It utilizes the Zeeman effect in vapor of alkali elements such as rubidium or cesium, which have only a single valance electron in the outermost energy level. If a polarized light-beam is shone at approximately at 45° to the magnetic field direction on the magnetometer in the presence of Earth's magnetic field the electrons precess about the field direction at Larmor frequency γ_e . At one part of the precession cycle an electron spin is almost parallel to the field direction, and one half-cycle later it is nearly antiparallel. The varying absorption causes a fluctuation of intensity of the light-beam at the Larmor frequency which is detected by the photocell and converted to an alternating current. By means of a feedback circuit the signal is supplied to a coil around the container of rubidium gas and a radio-frequency resonant circuit is created. The ambient geomagnetic field B_t that cause the splitting of the ground state is related by the Larmor frequency is given by

$$B_t = \frac{2\pi}{\gamma_e} f \quad (2.3)$$

Here γ_e is the gyromagnetic ratio of electron, which is known with an accuracy of about 1 part in 10^7 . It is about 1800 times larger than γ_p . So the precessional frequency is correspondingly higher and easier to measure precisely.

The sensitivity of an optically pumped magnetometer is very high, about 0.01nT, which is an order of magnitude more sensitive than flux-gate or proton-precession magnetometer.

Chapter 3

The Ethio-Finno Observatory (EFO)

The Ethio-Finno Observatory was established at 2004 in Ethiopia by researchers from Bahir Dar Universty and Addis Ababa University in Ethiopia, in collaboration with University of Oulu in Finland. The observatory is located north of Addis Ababa [09^o, 01' N, 38^o, 48' E, LT=UT+3h] around 7 km from the main city, on Entoto mountain at an altitude of nearly 2500 m from sea level. The main objective of the observatory to study the Earth's upper atmosphere phenomena using pulsation magnetometer assembly which is delivered by Oulu University Space Physics institute. The location of the observatory makes it ideal place to investigate ionospheric process like the Equatorial Electro Jet (EEJ), a narrow electric current flowing north-south above 100 km the ULF waves, and the Alfvén resonators wave which have not yet observed around the equator.

3.1 Instrumentations

3.1.1 Sensors at EFO

The pulsation sensors at EFO consists of the tri-axial pulsation magnetometer, the total length of 1.07m, the total diameter 7.5cm, and the total weight of 9kg. The length of the sensor is 1m. The prototype has a core diameter of 15mm and winding of 1,950,000 turns of 50 μ m copper. Aluminium and hard-paper are used in order to avoid eddy currents. The whole sensor is covered by a PVC-tube closed at the ends for water protection. A connector and an about 100m long plastic tube sensor

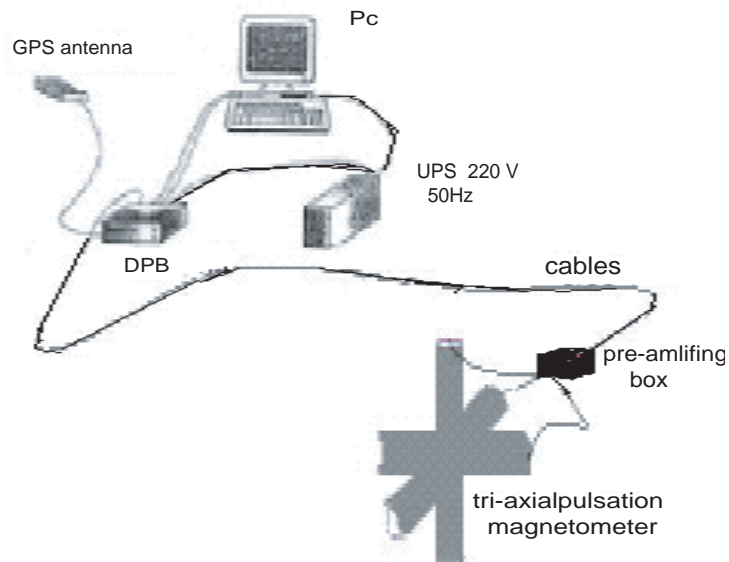


Figure 3.1: Instrumental setup of ionospheric monitoring at EFO triaxial pulsation magnetometer positioned on plane surface

cables lead to the analog to digital converter (ADC). The sensor configuration is designed to be installed on the Earth surface. The sensors are calibrated in such a way that the vector magnetic field along each three geomagnetic axes can individually be measured by sensors placed in the direction of the corresponding geomagnetic components (H, D, Z). The noise density of the sensor at 1Hz is $< 10pT/\sqrt{Hz}$ and offset at room temperature of $1nT$. Figure 3.1 shows the schematic diagram of the pulsation magnetometer at EFO.

3.1.2 Analogue Electronics

Analogue electronics perform the operations sample-and-hold, quantization and encoding. The combination of the quantizer and encoder is often called along to digital converter, this gives a time varying output. The sampler in the analog to digital converter (ADC) consists of sampler and holds device. The combination of the sampler, hold device and ADC accepts the analog signals from the pre-amplifying box and replaces it with a sequences of digitized symbols.

3.1.3 Digital Electronics

The digital electronic part of the magnetometer output (V_x , V_y and V_z), the three photometer result (C_x , C_y and C_z) are digitized continually by a 16 bit analog to digital converter at a rate of 100Hz. This makes it possible to get accurate information about field variations/pulsations up to 50Hz. The digital processing unit or board (DPU) controls the ADC board and the transmission of the raw data to the host Pc (Lab top) via a serial link. The digital data are transmitted in frames. One frame includes 100 field vector and additional housekeeping data like time and supply voltage.

A global positioning system (GPS) receiver is added to the DPU board in order to get the absolute time and have time synchronization to the data of other world wide observatories.

The power to the magnetometer is supplied through a single phase UPS which works with frequency of 50 or 60Hz. During interruption of of the main power the UPS is adjusted to supply power for one hour.

3.1.4 Host Pc

A standard Toshiba Pc (Lab top) is used as host computer. The software for data conversion, real time display and event detection. In addition and analysis like selectable data filtering, calculation of standard deviation etc. has been developed in Space Research Institute of Oulu University to process the pulsation magnetometer data. The software at the Pc manages the data reduction to an appropriate data rate and the storage of these data, what can also be done by command.

Chapter 4

Measurement and Data Analysis

4.1 Data from EFO and Observed Interference

The data collected from EFO pulsation magnetometer contains information of the three components disturbance of Earth magnetic field and the corresponding time. The data from each sensor is digitized at a sampling frequency of 100Hz (hundred sample per second) and are recorded on a hard disc for 24 hours. This enables the magnetometer to detect Earth's magnetic field disturbance in frequency band 0.01-50Hz.

In this study we proceed through analysis of the magnetic disturbance recorded four consecutive days, from February 15, 2005 to February 18, 2005 and on the data collected while experiment was conducted. This time was preferred because it was one of the quietest time in recent years. In addition amplitudes level of enhancement of the four days selected data as shown on figure 4.1 easily indicates that there are a lots of actions undergoing at EFO.

Very intensified amplitude enhancement begin on February 15-16, 2005 which proceed till to nearly 17 UT accompanied without intensified disturbance nearly until 06 UT of Feb 17. Then small level of amplitude enhancement when compared to February 15-16, 2005 has proceed till the end of Feb 18 except from 22 UT of Feb 17 to 03 UT of Feb 18. Clear observation of the disturbance enhancement in the amplitude three kind depending on the length of time of existence and the shape disposed. Figure 4.3 indicates first kind of disturbance which characteristically are

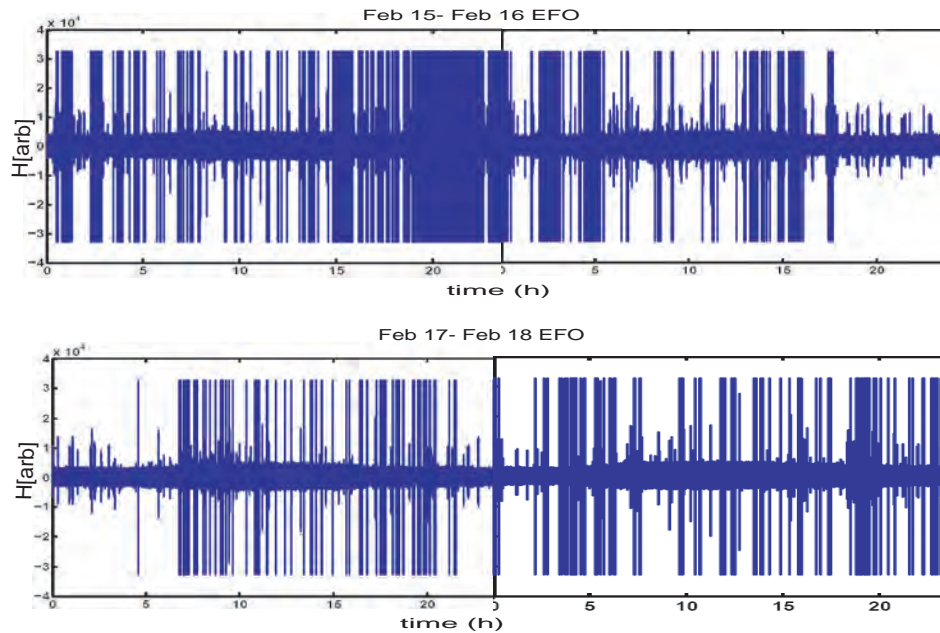


Figure 4.1: The H-component of the four days Feb 15-18, 2005 geomagnetic disturbance recorded at EFO.

very short quasi-periodic pulses which persists for less than 0.5 seconds. The second kind of disturbances shown in Figure 4.4 are quasi-periodic pulse as the first type with more amplitude enhancement and lasts with time less than 0.85 seconds. Figure 4.5 indicates the third kind of disturbances which are random in nature with very intensified amplitude level and lasting time of more than 1.0 seconds. From Figure 4.1 it is easy to see that disturbance of the first and the second kind are recorded in all four days with very large number in comparison to the third ones of our data. But the third kinds were more observed on the first and the last days. The effect of these magnetic disturbance can be easily determined from the background noise using a color code and frequency analysis.

The frequency content of the first one hour selected from each day is shown in Figure 4.2. Small hours are included because the computer we are using doesn't have sufficient memory to analyze too much routines and large size data. According to the figure the frequency region 0.01-10 Hz can be clearly observed with increasing interval 0.5 Hz to 1.0 Hz. The most pronounced spectral spikes are observed in the

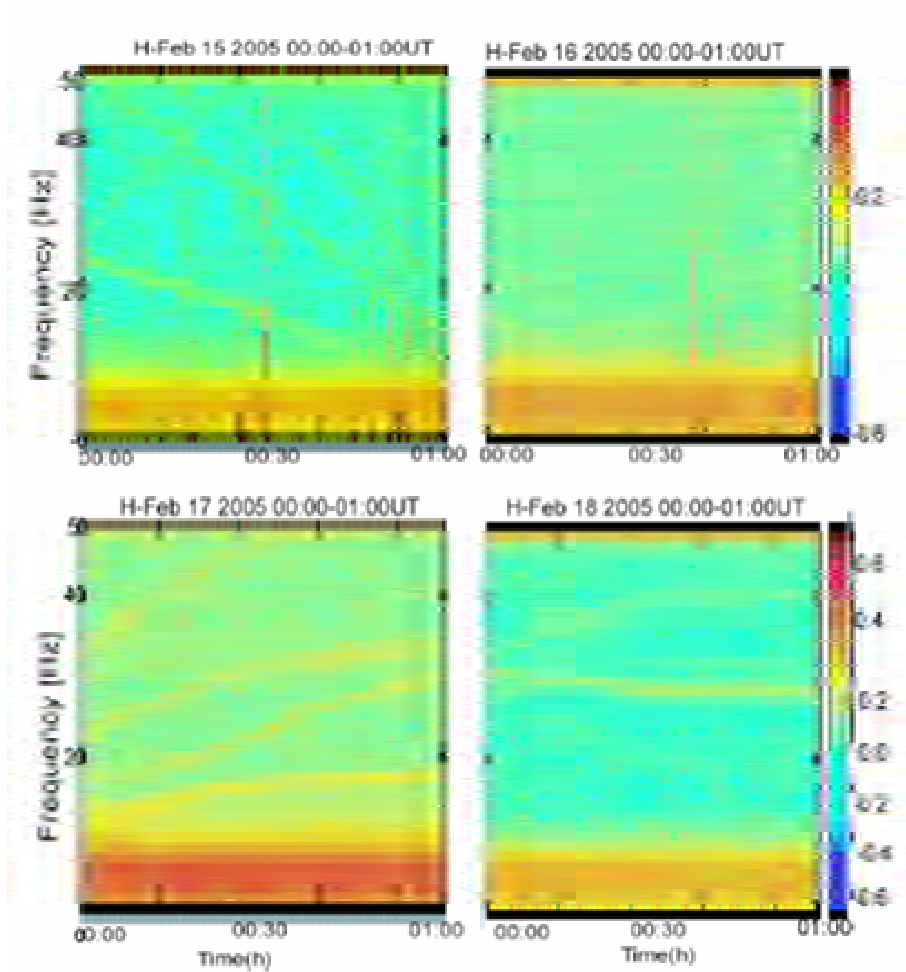


Figure 4.2: The dynamic spectrum in a color code as a function of frequency and time as observed at EFO from the first one hour of the four days. The ordinate displays frequency in Hz and the tick mark abscissa indicates the time. Deep red of the color code corresponds to plus ~ 0.6 and deep blue to minus ~ 0.6 .

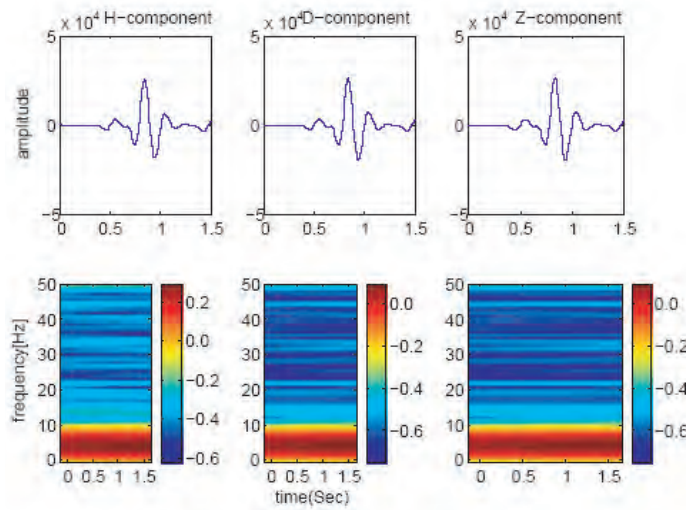


Figure 4.3: Three components of the quasi-periodic disturbances which persists for less than 0.5 seconds. The color code shows on the vertical axis frequency content and the horizontal axis time.

frequency range ~ 3 to ~ 5 Hz. Above off the short geomagnetic pulsation range, there are patterns of straight, up and down chirp wave forms which are intensified by yellow code. Some of the chirps have intensively high in the frequencies ~ 14.5 Hz, ~ 24 Hz, ~ 32 Hz. At the tips of the dynamic spectral analysis of the four hours there is a straight horizontal line dominated by reddish toned color at a frequency of 50Hz. In addition, it easy to see a sharp straight vertical lines for a short period of time which consists all frequency (0-50Hz) these are the results of strong enhanced disturbance like shown in Figure 4.4 and 4.5. To see characteristics and effect of the peak disturbance each of them spectral peaks were investigated.

First let's look at the spectrum of small quasi-periodic pulses Figure 4.3 taken for time less than 0.5 seconds. The frequency enhancement occurs 0.5-5 Hz. These characteristic spectral frequencies in regular bases are observed in all events recorded for such pulses. According to Figure 4.4 the dynamic spectra of random disturbance taken for 2 seconds it indicates that the disturbance consists all sort of frequency; the maximum allowed Nyquesit frequency. In order to fined out the cause of this intensified enhancement we continue by relating the solar and geomagnetic activities, performing different experiments to identify the effect of ferrous object and grounding current loops source.

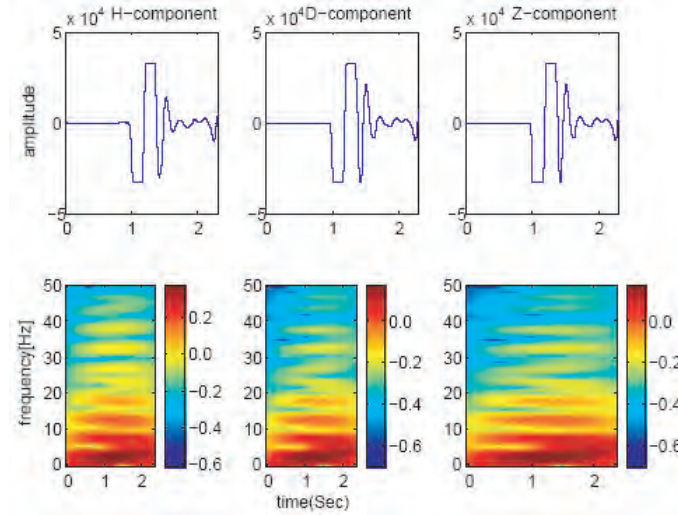


Figure 4.4: Three components of the sharp pulse quasi-periodic disturbances which persists for less than 0.85 seconds. The color code shows on the vertical axis frequency content and the horizontal axis time.

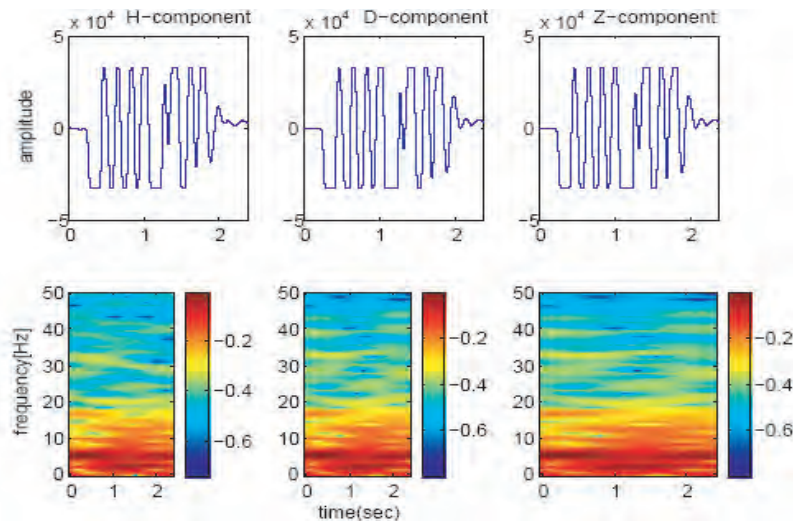


Figure 4.5: Sample of long persisting disturbances of the three components. The dynamic spectrum indicates the disturbance possess frequency 0-50Hz.

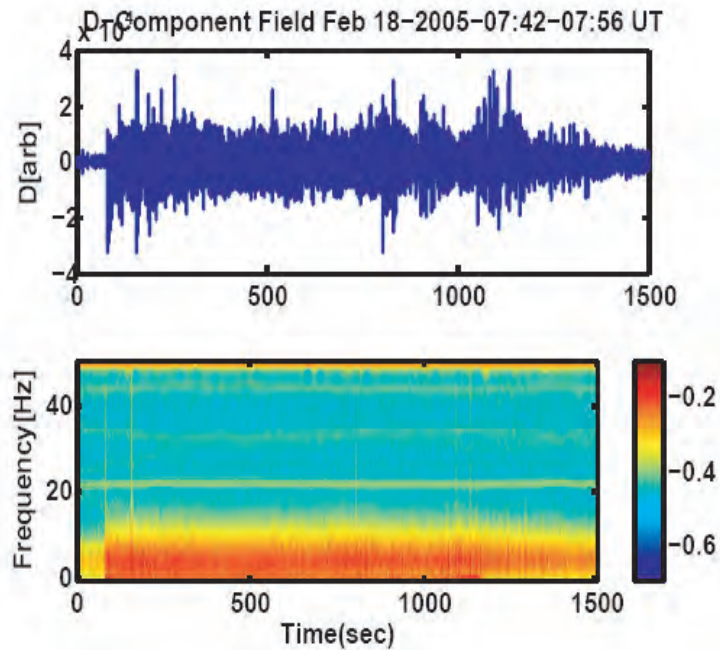


Figure 4.6: Upper panel: indicates disturbance on February 18, 2005 due to minor storm. Lower panel: is the frequency content of the disturbance in color code.

4.2 Investigations of the Possible Sources of the Interference

4.2.1 Solar and Geomagnetic Effect

According to the report of Royal Observatory of Belgium (22) solar and geomagnetic controlling center Feb 01-03 has only B-flares; during the period Feb 04-Feb 19 occasional C-flares were produced, culminating in the only M-flares of the month on Feb 19. No proton events occurred, but few halo CMEs were observed. This all attributes in showing no strong geomagnetic perturbations this month. Active conditions occurred on Feb 02-03, Feb 06-11, Feb 16-19 and Feb 05, with minor storms conditions from Feb 07-08 and on Feb 18.

The geomagnetic Dst value of the four days Feb 15-Feb 18 obtained from WDC-C2 Kyoto (23) is given in table 4.1. According to the table interplanetary magnetic field Feb 15 showed minor fluctuations approximately between ± 5 nT almost the whole day. The solar wind speed was between 350km/s and 400km/s. However

during the second half of Feb 16 were active conditions raised, possibly related to the arrival of the partial CME from Feb 13 (24). The interplanetary magnetic field showed fluctuations approximately between ± 5 nT. The solar wind speed was falls from 420km/s to 380km/s. After quiet period on Feb 17 on Feb 18 the solar wind speed rose from 450km/s to 600km/s with maximum -20nT shift on the geomagnetic value which result a minor storm conditions.

Day	Time=number of hour UT day, DST value in unit=nT																							
	1	2	3	4	5	6	7	8	9	10	11	12	13	14	15	16	17	18	19	20	21	22	23	24
Feb 15	-19	-18	-17	-15	-13	-12	-11	-9	-7	-5	-4	-3	-4	-7	-10	-10	-8	-8	-10	-10	-14	-8	-4	-8
Feb 16	-8	-10	-3	-9	-7	-8	-8	-10	-7	-7	-1	-1	-13	-24	-35	-41	-49	-55	-54	-44	-41	-32	-32	-33
Feb 17	-24	-22	-23	-28	-29	-25	-24	-24	-21	-19	-17	-19	-20	-20	-18	-17	-23	-20	-18	-15	-20	-24	-20	-19
Feb 18	-46	-80	-86	-78	-75	-69	-67	-63	-51	-49	-54	-56	-48	-44	-51	-53	-45	-47	-41	-37	-42	-41	-41	-42

Table 4.1: The Dst values of four days from Feb 15-Feb 18, 2005 (22).

According to Figure 4.1 on Feb 15 and 16 the perturbation level is very high despite low geomagnetic activities were recorded. Further more despite increment of geomagnetic Dst value highly after the second half of Feb 16 the disturbance level recorded is almost similar with Feb 15 of the same period which in the contrary possess comparably very low geomagnetic index Dst value. The increment of the Dst value and occurrence of minor geomagnetic storm of Feb 18, 2005 was recorded by the D-component of the magnetometer and the corresponding dynamic spectrum nearly for twenty minutes as indicated in Figure 4.6. The figure clearly indicates amplitude enhancement or disturbance level produced and the frequency content is not the same as strongly enhanced peaks effects as in Figures 4.3, 4.4, and 4.5. The dynamic spectrum verifies the disturbance of minor storms or geomagnetic and solar activities creates more geomagnetic pulsation in ULF bands. This manifests that the interference in EFO are not initiated by solar and geomagnetic activities in the upper polar atmosphere.

4.2.2 Effect of Ferrous Objects

The location of the sensor makes it susceptible to a disturbance vibrating, moving and stationary ferrous objects. The sensors are surrounded by iron made fence which is close up to less than two meter. Furthermore spherical weather radar nearly at a

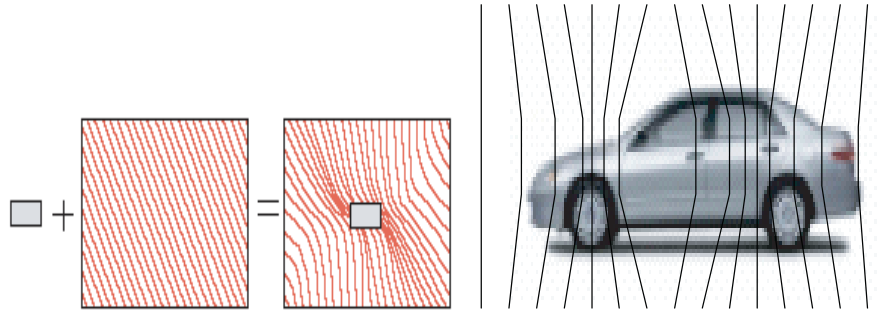


Figure 4.7: Ferrous object disturbance in uniform field.

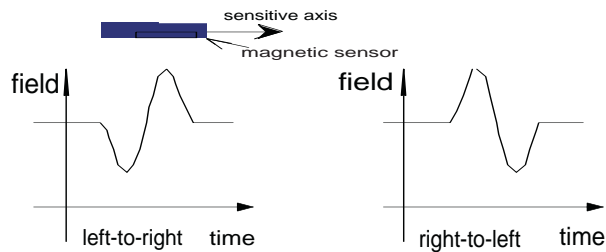


Figure 4.8: Direction sensing for ferrous disturbance moving over magnetic sensors.

distance of 30 meter and a satellite dish at 40 meter, long power line, vehicle main road which transports more than 400 cars of different kind in a single day that is located at a distance less than 300 meter and sub road that takes to the observatory.

From section 1.1.3 we have discussed that how magnetized and magnetic substance can cause a disturbance on Earth's magnetic field. For delving out the kind of effect ferrous object dispose on the shape and level of disturbance, we base our analysis on some experiments and works performed by other researchers.

When a ferrous object is vibrating or placed in a region where the sensor is sensitive the net result is characteristic distortion, or anomaly. If it is the Earth's magnetic field line of flux will be drawn towards the ferrous as in Figure 4.7. If the ferrous moves forward in the sensor direction the filed lines initial values will show in negative direction as in Figure 4.8. When the ferrous moves away from the sensor, the flux lines are attracted towards the ferrous which result a positive initial increase in the sensor out put as in Figure 4.8. Similar situations were observed during atmospheric

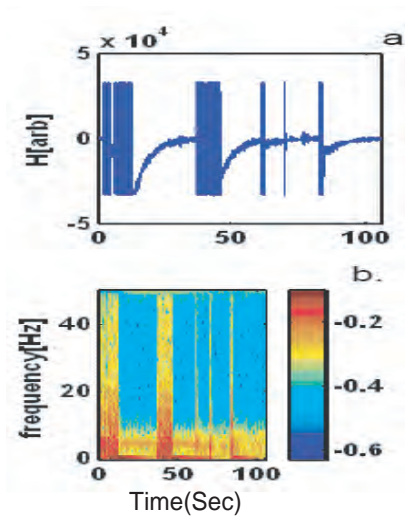


Figure 4.9: Disturbance created during the vibration of the wire fence near the sensors.

wind speed changes drastically which is sufficient enough to make vibration of the loosely tightened wire of the fence. Figure 4.9 shows the disturbance created when the wire fence is allowed to vibrate in small oscillation. The amplitude enhancement and the frequency spectrum shows as similarity to that of long persisting interferences observed in EFO.

The next analysis considers influence of vehicles that passes at the vicinity of the observatory. According to (15) and (16) magnetic field device measuring anisotropic magnetostrictive (AMR) serves to detect the disturbance from vehicles; effects of dipole magnets that emerges the combined effects of the engine, wheel location, rooftop, trunk locations and speed.

Being the observatory located at the tip of Entoto mountain which barley have an open plate ground makes impossible to test vehicle effect directly and associate with the disturbance. However, it is possible to analyze indirectly to sort out the effect by interrelating disturbance peaks number of different time with the recorded time (15). This works for EFO because the number of cars that use the nearby roads is not uniform through out 24 hours. During the local morning time 6-9 UT and in the local afternoon 16-19 UT very high number of cars are registered. In the local evening 20-05 UT very low and average number of cars from 09-16 UT. In contrast to what is expected for instance nearly from 20 UT of Feb 15 to 06 UT of Feb 16

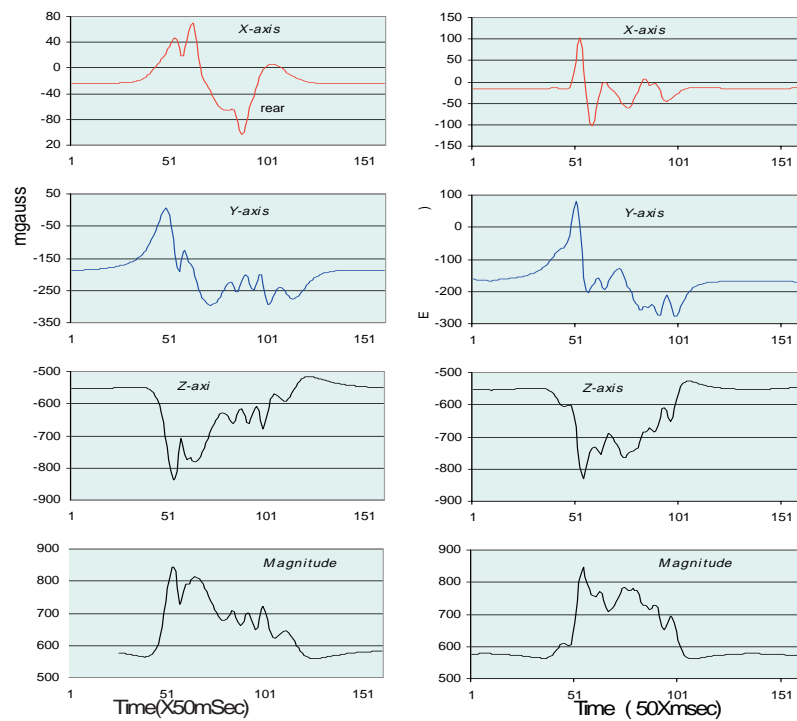


Figure 4.10: Left column indicates Earth's field variations for car (silhouette) driving over the magnetometer. Right column is due to car (saturn). Both vehicle are travelling in the same direction (16).

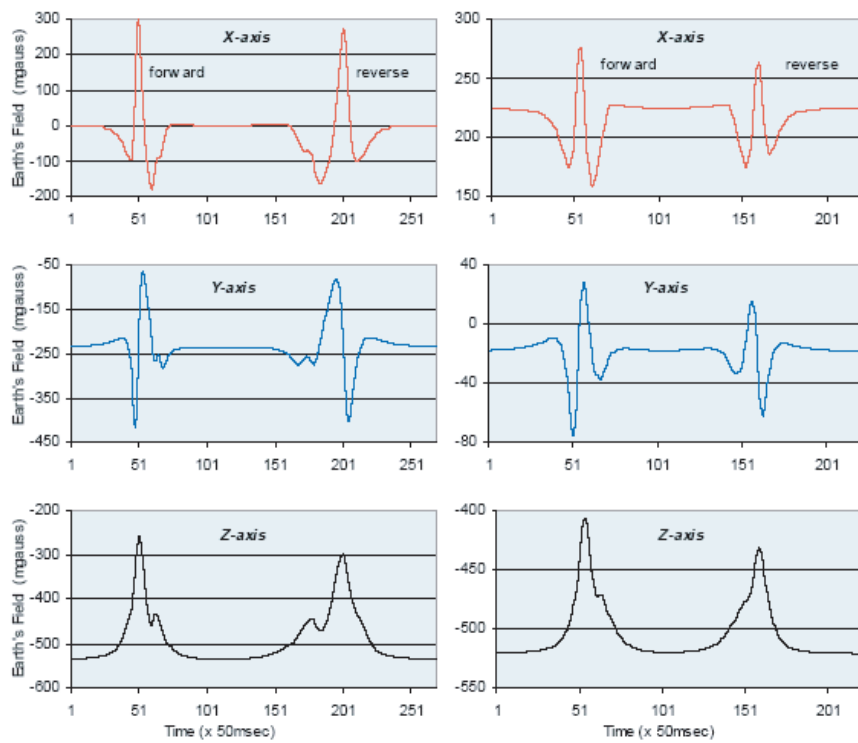


Figure 4.11: Left column the X, Y, and Z magnetic variation from a car in the forward (south) and reverse (north) and right column forward (west) revers (east) direction (16).

peak disturbance number recorded are very much larger than the possible number of vehicles that passes near the observatory. This gives a clue that vehicles responsibility to cause strong enhanced disturbance is rare.

Other way of vehicle influence determination is to relate the shape of the disturbance (16). Figure 4.11 shows the shape of disturbance that is observed using two different vehicles (16). The difference curve for different vehicle indicates that each small section of the car produce a repeatable signature variation of the Earth's field that is specific to a given vehicle. Dissimilarity of the three axis is an indication for the body of the vehicles effects each axis a little differently. In contrast this relation expected the shape of the disturbance at EFO almost all shows similarity and all the three component shows the same character. Furthermore again studies by (16) explains disturbance produced by vehicles moving towards and away (left to right and right to left) have different characteristics of shape and phase information as seen in Figure 4.13. But almost all the disturbance in EFO we are interested to know the source shows characteristics as in vehicles moving towards the sensor, which is one direction traffic flow that is not really happening on the nearby roads. Thus it is possible to suggest vehicles travelling near the observatory barely produces strongly enhanced interference we are observing.

4.2.3 Errors from Ground Loop Effect

The NEC, National Electrical Code, defines grounding as: " a conducting connection, whether intentional or accidental between an electrical circuit or equipment and the Earth, or to some conducting body that serves in place of the Earth." (25) Grounding are two types, Earth grounding and equipment grounding. Earth grounding is an intentional connection from a circuit conductor usually the neutral to a ground electrode placed in the Earth. Equipment grounding is to be ensure that operating equipment within a structure is properly grounded. These two grounding systems are required to be kept separate except for connection between the two systems to prevent differences in the potential from possible flashover from a lightning strike. The purpose a ground besides the protection of people, plants and equipment is to provide safe path for the dissipation of fault currents, lightning strikes, static discharge,

electromagnetic influence (EMI), and radio frequency influence (RFI) signals and interferences.

Despite grounding solves many problems, but it can cause new ones. One of the most common problem is ground loops. A ground loop can occurs when there is more than one ground connection path between the two pieces of equipment. The duplicate ground path from the equivalent of a loop efficiency picks up interference currents. these currents are changed into voltage functions. As a consequence of ground loop induces voltage, the ground reference in the system is no longer a stable potential, so signals ride on the. The noise becomes part of the program signals.

A ground loop in the power or signal can occur also when some components in the same system are not receiving its power from a different ground than other components, or the ground potential between two pieces of equipment is not identical. Usually a potential difference in the ground causes a current to flow in the interconnects. This intern modulates the input of the circuitry and is treated like any other signal feed through the normal inputs. Figure 4.12 shows an example situation where two ground equipments are interconnected through signal wire ground and the main ground wire. In this situation there is 1A current flowing in the wire causes 0.1V voltage difference between those two equipment grounding points.

In EFO ground loop problem is suspected because some of the equipments are linked with shielded cable which are quite likely to face some problems. Currents could quite run from one piece of equipments, into the Earth cable, into another piece of the equipment, then back to the first piece via a shielded sensors cable. If there is any current flowing in any wires, there is some potential difference which causes current to flow in other wires also which causes problems. The loop will also acts as coil and pick currents from the changing Earth magnetic fields around it. Wire loops acts also like an antenna picking up radio signals which are sent for the radio signal receiving satellite dish in the observatory. The result is that unwanted signals recording in EFO data.

Experiments were conducted on the components of the observatory if the disturbance emanate from grounding current loops from the near by materials. This was done by moving(shaking) the divider and unplugging the power cable to the PC. This

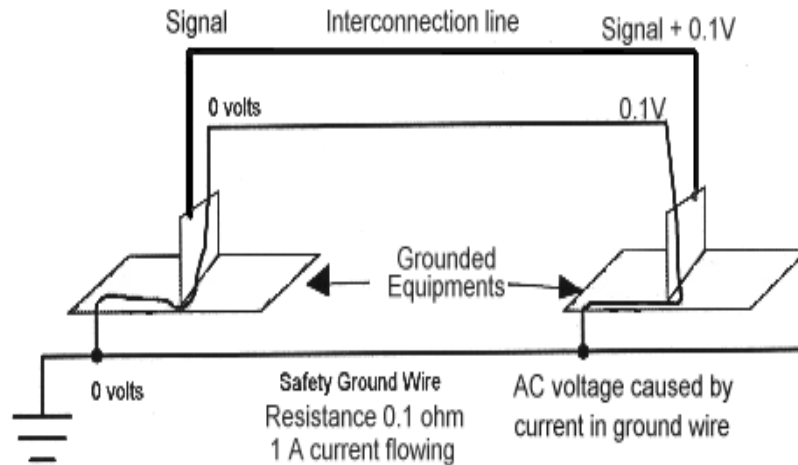


Figure 4.12: A simplified ground loop producing circuit.

two process creates sharp (impulse) signal as seen in Figure 4.13 if grounding current loops doesn't exist in any part of the observatory components. To identify if the grounding error is close through the UPS, first we disconnect the main from the UPS so that all the systems obtain power from the UPS alone. Then we move the divider a little bit and these have created a strong impulse as in Figure 4.14 which implies the harmful grounding current loops are not closed through the UPS. The same experiment was repeated after reconnecting the UPS with the main by changing the polarity of the UPS and the same situation was observed.

Second experiment conducted to search out if there is grounding current loops sources are near to the sensors. This was done by allowing all the system to gain power only from the UPS. Then we disconnect the system from the home made grounding. Unplugging the power cable after the divider have created a strong impulse. Finally we connect the home made grounding to the system and place a glass sheet under the pre-amplifier box expected strongly enhanced disturbances are not observed see Figure 4.15 the same situation repeated while unplugging the power to the PC. Finally we let a person standing on the ground keep firmly the pre-amplifying box in its hand and similarly intensified disturbance as in Figure 4.14 are repeated. Which is indicating the grounding current loops are existing near to the sensor. Hence the disturbance at EFO we are interested emerges due to grounding current loops

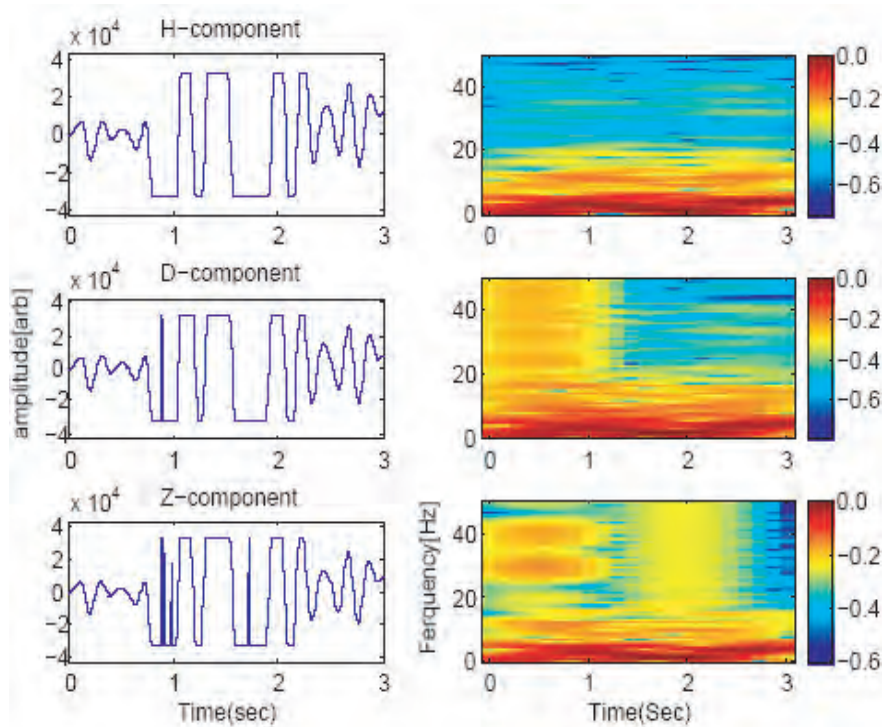


Figure 4.13: A sharp pulse created while moving the divider or unplugging the power cable after the divider. This is the disturbance expected if the grounding current loops doesn't exist in close the magnetometer and its parts.

near the sensors.

The other evidence which support the cause of pick disturbance in EFO as the ground current loop is that all the disturbance have similar phase information which is the signals are linearly polarized. This because equal amount of potential difference (voltage) is incorporated to the wires (cables) that link the sensor and the other components.

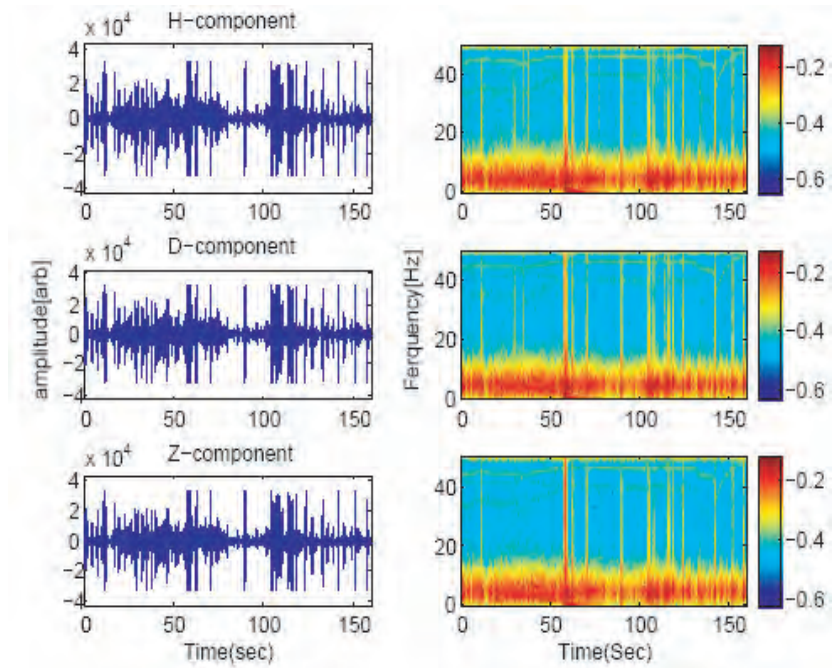


Figure 4.14: Observed disturbance and corresponding frequency content during grounding current loops source test is held near the UPS.

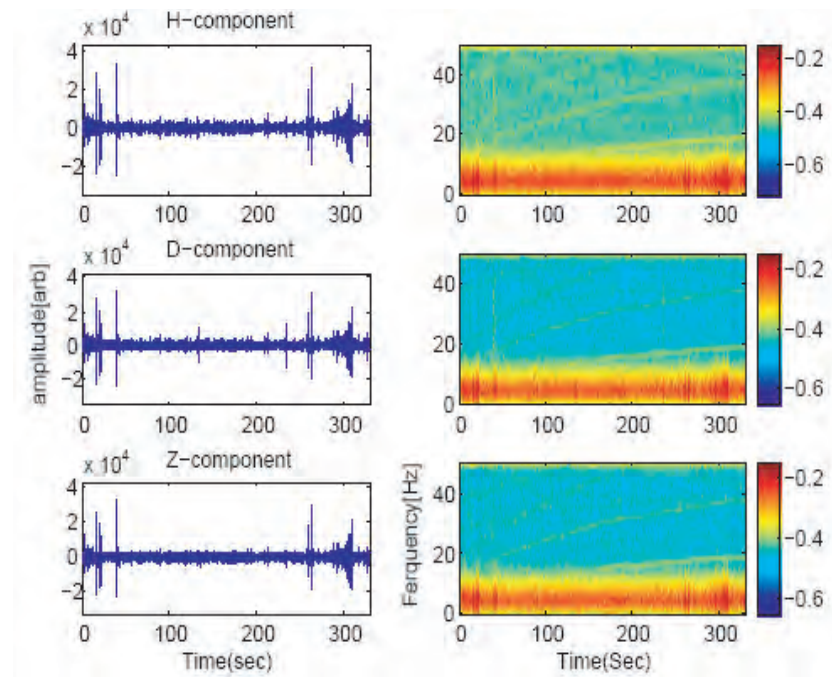


Figure 4.15: Observed disturbance and corresponding frequency content while grounding current loops source test is held near the sensors.

Chapter 5

Conclusions

This study carefully examines the disturbance observed in Ethio-Finno Observatory. We find out that the disturbance observed are contributions of the upper polar atmospheric process, the local sources close to the observatory and near the sensors. We have examined the possible sources of strong enhancement and have found that strong motions of ferrous objects specially the wire fence near the sensors and grounding current loops close to the sensors are responsible. In addition the frequency code tells long persisting reddish toned at 50Hz in the dynamic spectrum is as the data is corrupted by the interference from the nearby power line.

Despite these local effects are corrupting the recorded data as strong and weak interference, the observatory location essentially supplies grate deal of information of the earths magnetic field. The minor storm recorded on Feb 18 2005, the quasi-periodic disturbance which are the result of high frequency (HF) radio waves, spectral spikes ~ 3 to ~ 5 Hz are Pc 1 type magnetospheric emissions. Frequencies ~ 14.5 Hz, ~ 24 Hz, ~ 32 Hz are Schumanns (global) resonance harmonics have been observed in the four days data.

Chapter 6

Future directions

Based on the analysis of this thesis, it is clear that the data at EFO is corrupted by disturbances in a pronounced manner from local sources which is not desired for the very basic aim of the observatory. In order to gain optimum out come during the future work of the magnetometer or to maximize the information gained from the natural disturbance of earth's magnetic field in the observatory prominently one have identify the actual source of the grounding current loops. In addition the ferrous materials which are located near to the sensors must be removed.

Moreover in this work we have based ourself on references by other researchers in order to see the contribution of vehicle on EFO data. For better analysis, one has to carry on real time experiment by using a portable magnetic field measuring devices if there exists attribution of magnetic anomalies from the nearby flowing vehicles.

In addition we haven't come acrose the impulse response of the pulsation magnetometer, which tells if there are false parts or bad design. So it is essential to determine the impulse response analysis.

Bibliography

- [1] Primdahl, F.,: The fluxgate magnetometer, *J. Phys. E : Sci. Instrum.*, Vol. 12. 1972.
- [2] Bruce A., Buffett.,: Earth's Core and the Geodynamo, *Science Vol.* 288, 2000.
- [3] Jacob J. A., Russell R. D., Wilson J. T.,: *Physics and Geology* , McGraw-Hill, New York, 1974.
- [4] Olsen W. P.,: Intro to the topology of magnetospheric current systems, in magnetospheric currents, ed. Potemra, T. A., *Am. geophys. Un. Mongr.*, 28, 1984.
- [5] Volland, H.,: *Atmospheric Electrodynamics*, Springer-Verlag, Berlin. pp. 1-205, 1984.
- [6] Olsen, N.,: A model of the geomagnetic field and its secular variation for epoch 2000 estimated from rsted data, *Geophys. J. Int.* 149, 454 – 462, 2002.
- [7] Langel, R. A., and Hinze, W.J.,: *The Magnetic Field of the Earth,s Lithosphere: The Satellite Perspective*, Cambridge University Press, Cambridge, pp. 1-429, 1998.
- [8] Hollerbach, R.,: On the theory of the geodynamos, *phys. Earth planet. Inter.*, 98, 163 – 185, 1996.
- [9] Brekke, A.,: *Physics of the upper polar atmosphere*, John Eiley and Sons Ltd., 1997.
- [10] Landsberg,H. E., Miegghan,J. Van.,: *Advanced in Geophysic Academic Press*. New York, Vol. 13 pp. 5, 1996.
- [11] Feynman, J., and Gabriel, S. B., P. C.,: On space weather consquences and predictions, *J. Geophys. Res.* 105, 10, 543 – 10, 564, 2000.

- [12] The New Encyclopaedia Britannica, 15th Ed. Vol. 17, Encyclopaedia Britannica Inc pp. 591, 1992.
- [13] Parkinson, W. D.,: Introduction to Geomagnetism, Scottish Academic Press. Edinburgh pp. 433, 1983.
- [14] Olsen, N.,: Magnetospheric contributions to geomagnetic daily variations, *Ann. Geophys.*, 14, pp. 538 – 549, 1996.
- [15] Ding, J., Cheung, S.-Y., Tan, C.-W., Vaniya, P.,: Signal Processing of Sensor Node Data of Vehicle Detection, *IEEE*, pp. 1 – 6, 2004.
- [16] Caneso, M. J., Withanawasam, L. S.,: Vehicle Detection and Compass Applications Using AMR Magnetic Sensors. Honeywell SSEC, 2004, < [http : //www.ssec.honeywell.com](http://www.ssec.honeywell.com) >.
- [17] Onwumechilli C. A., and Ozoemena, P. C.,: Contours of equatorial electrojet current density, *J. Atmos. Terr. Phys.* 51, pp. 163 – 168, 1989.
- [18] Potemna, T. A.,: Birkerland Current; Presents Understanding and some remaining questions, in *High – latitude space plasma physics .eds* Hultqvist, B., and Hagfors, T., *Noble Symposium*, 54. Plenum, New York, 1982.
- [19] Maeda, h., Iyemon, T., Araki, T. and Kamei, T.,: New evidence of a meridional current system in the equatorial ionosphere, *Geophys. Res. Lett.* 99. 337 – 340, 1982.
- [20] Giglielmi, A. V., and Pokhotelov O. A.,: Geoelectromagnetic Waves, Institute of physics Bristol, 1996.
- [21] Lowriner, W.,: Fundamentals of Geophysics, Cambridge University Press, Cambridge, 1995.
- [22] Solar Influence Data analysis center, : Monthly summary of solar and geomagnetic activities, 2005.
< [http : //sidc.oma.be](http://sidc.oma.be) >.
- [23] Kyoto University, : Hourly equatorial Dst values, 2005.
< [http : //swdwww.kugi.kyoto – u.ac.jp](http://swdwww.kugi.kyoto-u.ac.jp) >.

- [24] The Austaralian Space forecasting Centre,: IPS Solar and Geophysical Report, 2005,
< <http://www.asfc@ips.gov.au> >.
- [25] Engdahl, T.,: Ground loop problems and how to get rid them, ELH. con communication Ltd., 2005,
< <http://www.epanorama.net> >.